Enhanced photocatalytic activity of titanium dioxide by nut shell carbon

Xiaoliang Shi [a,b,*], Sheng Wang [b], Xuebin Dong [b], Qiaoxin Zhang [a,b]

[a] School of Mechanical and Electronic Engineering, Wuhan University of Technology, 122 Luoshi Road, Wuhan 430070, China
[b] State Key Laboratory of Advanced Technology for Materials Synthesis & Processing, Wuhan University of Technology, 122 Luoshi Road, Wuhan 430070, China

ARTICLE INFO

ABSTRACT

Nut shell carbon (NSC)–nanotitanium dioxide (TiO_2) composites were prepared by sol–gel method. Photocatalytic activity on degradation of dye Rhodamine B was studied. X-ray diffraction, field emission scanning electron microscopy, Brunauer–Emmett–Teller surface area, pore size distribution, ultraviolet–vis light absorption spectrum, and photoluminescence spectrum were carried out to characterize the composite catalyst. The results indicated that the photocatalytic activity of NSC–nano-TiO_2 composites was much higher than P25 (Degussa). NSC could greatly absorb the organic substance and oxygen of solution because of its large surface area.

1. Introduction

In recent year, titanium dioxide (TiO_2) has been widely studied owning to its application in photocatalysis [1], photovoltaic device [2], solar cell [3] and hydrogen production [4]. It is one of the most attractive semiconductors for photocatalysis. However, the property of TiO_2 is not enough for industrial purposes. TiO_2 is a wide band-gap semiconductor (3.2 eV), which only responds to ultraviolet light [5]. The photogenerated electron/hole pairs easily recombine, which reduces the photocatalytic activities [6]. TiO_2 is difficultly recycled after the reaction [7]. Several methods have been attempted to improve the photocatalytic efficiency [8]: (I) the generation of nanosized particles [9], (II) surface modifications improving the charge transfer efficiency [10], (III) ion incorporation improving the optical absorption properties [11,12], (IV) the immobilization of a highly active system [13,14].

Surface area of catalyst is a great importance for its catalytic performances [15]. Porous materials are of the best candidates for the preparation of catalyst materials with larger surface area. Several porous materials were used to improve the surface area [16,17]. Nut shell carbon (NSC) is a porous material and its surface area is extremely large. At the same time, NSC is easily recycled after the reactions.

In this study, NSC–nano-TiO_2 composites were synthesized by sol–gel method. The effects of NSC on photocatalytic activities were studied by destructing dye Rhodamine B. The conventional TiO_2 (P25, Degussa) was studied for comparison. To the best of our knowledge, this work may be the first report about utilizing NSC to enhance TiO_2 as photocatalyst. Dye Rhodamine B is a kind of typical azo dye, and its structure is shown in Fig. 1. The results indicated that NSC–nano-TiO_2 composites had much higher photocatalytic activity than P25.

2. Experimental

2.1. Materials

The dye Rhodamine B was purchased from the No. 3 reagent factory of Shanghai. Tetrabutyl titanate was got from the total reagent factory of Tianjing. All of the chemicals were analytical grade. NSC was got from Nantong Yongtong Environmental Protection Science and Technology CO., LTD.

2.2. Preparation of NSC–nano-TiO_2 composites

To prepare the NSC–nano-TiO_2 composites, butyl titanate and NSC were used as starting materials. $Ti(OR)_4$, H_2O, ROH and HNO_3 with the molar ratio of 1:1.5:20:0.16 [18] were homogenized by a magnetic stirrer until uniform sol was formed. NSC was put into the sol, and the mass ratio of TiO_2 and NSC was 5:100. At the same time, the mixture was stirred by a magnetic stirrer for 4 h and then dispersed by ultrasonic vibration for 2 h. The mixture was kept at

* Corresponding author at: School of Mechanical and Electronic Engineering, Wuhan University of Technology, 122 Luoshi Road, Wuhan 430070, China. Tel.: +86 27 87651793; fax: +86 27 87651793.
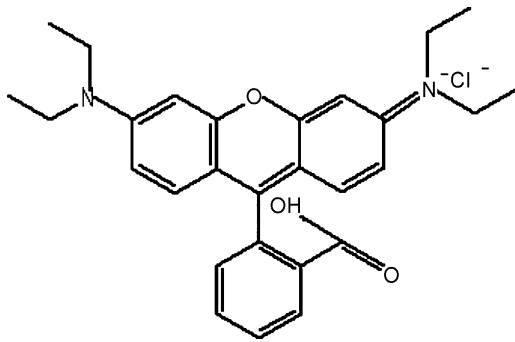*E-mail address:* sxl@whut.edu.cn (X. Shi).

Fig. 1. The structure of dye Rhodamine B (chemical formula = $C_{28}H_{31}ClN_2O_3$).

Fig. 3. XRD patterns of NSC–nano-TiO$_2$ composites and P25.

25 °C until it formed uniform gel. To obtain NSC–nano-TiO$_2$ composites, the gel was dried in an oven at 60 °C, and then calcined at 400 °C for 2 h in air.

2.3. Characterization

The as-prepared NSC–nano-TiO$_2$ composites and P25 were identified by X-ray diffraction (XRD) analysis using D/MAX-IIIA X-ray diffractometer (Japan). The morphology, particle size and structure of NSC–nano-TiO$_2$ composites were characterized by a S-4800 field emission scanning electron microscope (FESEM). Brunauer–Emmett–Teller (BET, Gemini 2360, MICRMERITICS) was used to measure the surface areas of samples. The pore size distribution was characterized by an automatic mercury porosimeter (AutoPoreIV9510, Americian). The absorption spectra of samples were obtained with an ultraviolet–vis (UV–vis) spectrophotometer (Varian CARY 5000, Australia) between 200 and 800 nm. The photoluminescence spectra were recorded with a Shimadzu RF-5301 fluorescence spectrophotometer.

2.4. Photocatalytic experiments

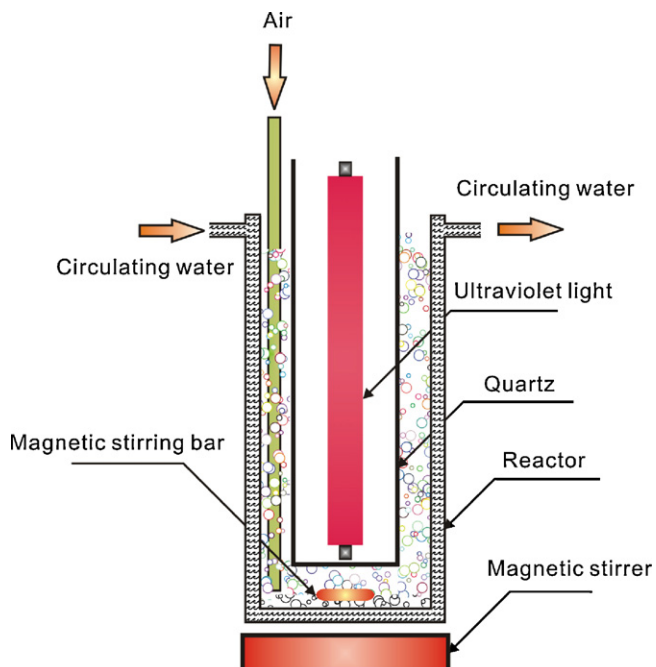An equipment of 300 ml capacity was used as a photocatalytic reactor. The equipment was a cylindrical container including three layers. The middle was the reactor, and the outer was a tube for cooling water. The schematic diagram of photocatalytic reactor was shown in Fig. 2. The temperature of the reactor was maintained at room temperature by circulating water. Air was bubbled by a fan to keep enough oxygen ambient. And a pump was used to make the reactants fully contact with each other. The initial dye Rhodamine B concentration was 100 mg/l. The dosage of TiO$_2$ was 0.3 g. And the
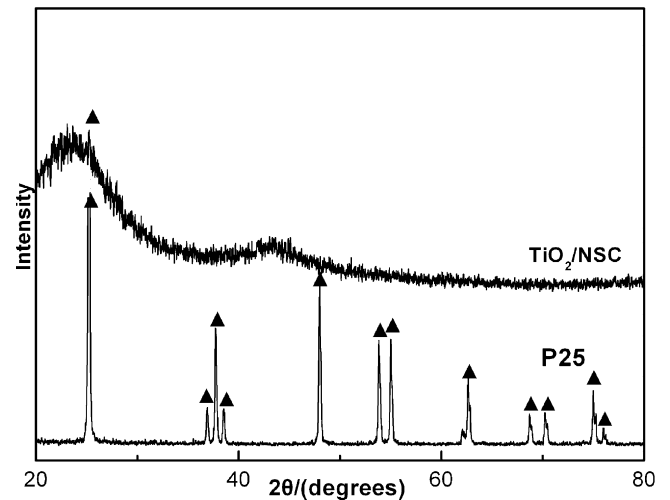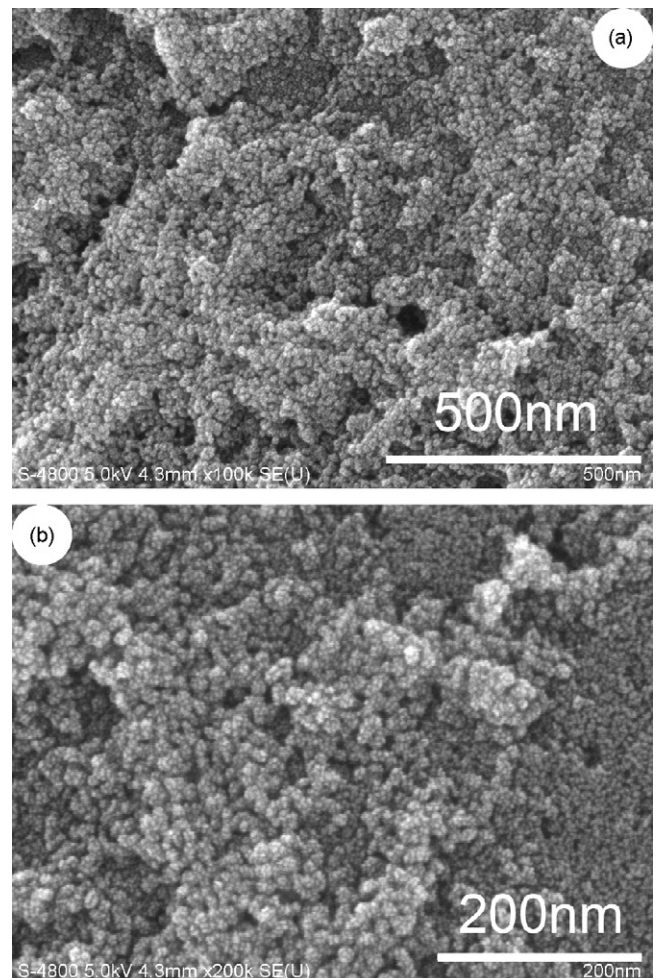

Fig. 2. The schematic diagram of photocatalytic reactor.

Fig. 4. FESEM micrographs of NSC–nano-TiO$_2$ composites.

Table 1
BET surface areas of samples.

Sample	BET surface area (m^2/g)	Particle size (nm)	Average pore size (nm)
NSC–nano-TiO$_2$ composites	921.5386	–	68.1
TiO$_2$	234.375	10	–
P25	56.4958	27	–

*BET surface area: $s = 6/(d \times \rho)$. (d = diameter; ρ = density).

same dosage of TiO$_2$ was used in NSC–nano-TiO$_2$ composites. To get to the balance of adsorption and desorption, the reaction was carried out at dark room for 90 min. Then the reactants were irradiated by an ultraviolet lamp (λ = 365 nm). The samples were taken every 15 min, centrifuged and filtrated, orderly. The dye was analyzed on an UV–vis spectrophotometer with the maximum absorption wavelength of dye Rhodamine B at 554 nm [19].

3. Results and discussion

3.1. XRD analysis

The XRD patterns of NSC–nano-TiO$_2$ composites and P25 are shown in Fig. 3. Only the most intensive peak of nano-TiO$_2$ was visible in the XRD pattern of NSC–nano-TiO$_2$ composites, as shown in Fig. 3. Other peaks of nano-TiO$_2$ are covered by the pattern of NSC. The results indicate that the peaks of nano-TiO$_2$ would not become visible when the mass ratio of nano-TiO$_2$ and NSC is low.

3.2. FESEM analysis

FESEM micrographs of NSC–nano-TiO$_2$ composites are given in Fig. 4. TiO$_2$ nanoparticles are uniformly distributed on the surface of NSC, as shown in Fig. 4. The average particle diameter of nano-TiO$_2$ is about 10 nm. The grain size distribution of nano-TiO$_2$ nanoparticles is uniform. The images evidence that pores existed in the NSC–nano-TiO$_2$ composites.

3.3. BET surface area and pore size distribution analysis

The BET surface areas of P25 and NSC–nano-TiO$_2$ composites are shown in Table 1. As shown in Table 1, the BET surface area of P25 is 56.4958 m^2/g, while the BET surface area of NSC–nano-TiO$_2$ composites is 921.5386 m^2/g. The BET surface area of NSC–nano-TiO$_2$ composites is nearly 15 times larger than P25. If the BET surface area of nano-TiO$_2$ (ca. 10 nm) is calculated by the formula [$s = 6/(d \times \rho)$]
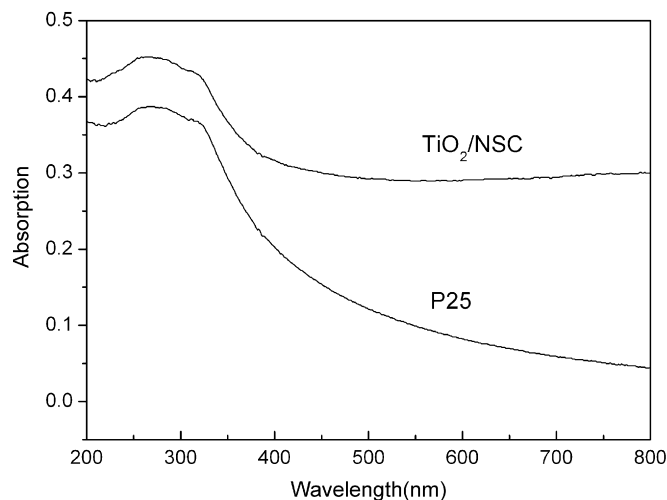

Fig. 6. UV–vis spectra of NSC–nano-TiO$_2$ composites and P25.

[20], the value is 234.375 m^2/g. And the P25 average particle size is about 27 nm. The results indicate that the BET surface area is greatly increased when nano-TiO$_2$ particles are supported by NSC. The pore size distribution of NSC–nano-TiO$_2$ composites is given in Fig. 5. As shown in Fig. 5, the main pore size range is below 1000 nm, especially between 200 and 1000 nm. The average pore size is about 68.1 nm, as shown in Table 1. The large BET surface area could be attributed to abundant pores of NSC.

3.4. UV–vis and PL spectrum analysis

The UV–vis absorption spectra of NSC–nano-TiO$_2$ composites and P25 are shown in Fig. 6. NSC–nano-TiO$_2$ composites exhibit stronger absorption than P25. The UV–vis absorption peaks of NSC–nano-TiO$_2$ composites are nearly the same with P25, and both of them lie in the ca. 265 nm. The blue-shift may be attributed to the surface effects and the quantum-size effects [18]. In order to study the effects of NSC on the recombination of e^-/h^+ produced by nano-TiO$_2$, the PL spectra are detected for NSC–nano-TiO$_2$ composites and P25. The PL spectrum of NSC–nano-TiO$_2$ composites shows one intense narrow emission bands at λ_{em1} = 471 nm, when NSC–nano-TiO$_2$ composites is excited by ultraviolet light with λ_{ex} = 265 nm, as shown in Fig. 7(a). The PL spectrum of P25 shows two intense emission bands at λ_{em2} = 408 and λ_{em3} = 475 nm, when P25 is excited
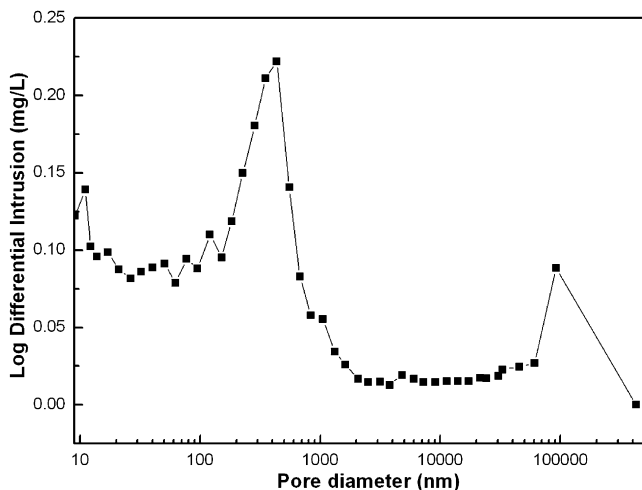

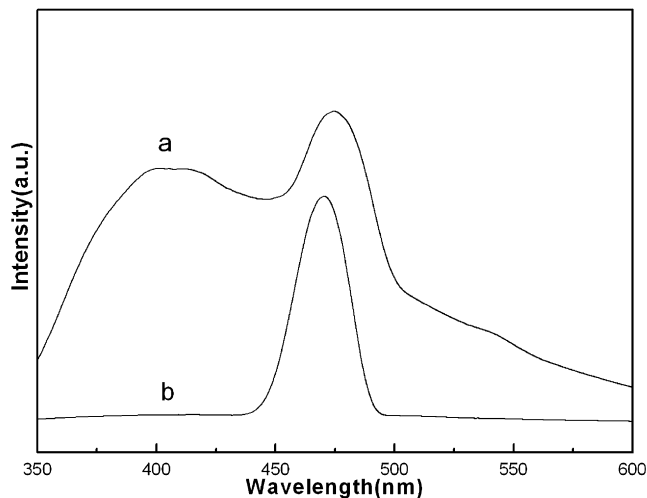**Fig. 5.** The pore size distribution of NSC–nano-TiO$_2$ composites.

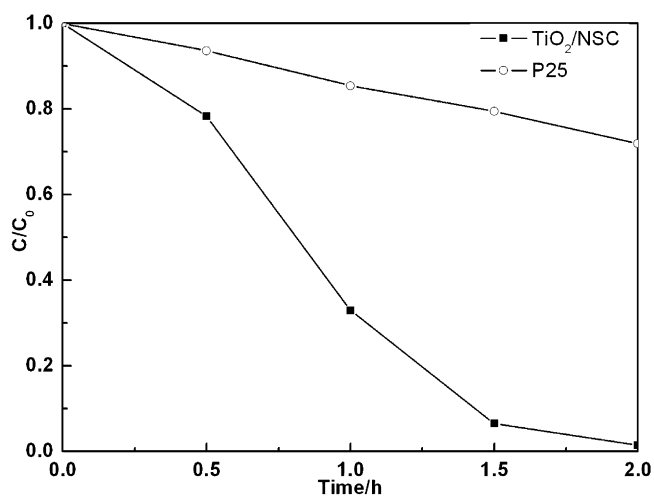**Fig. 7.** Photoluminescence spectra of NSC–nano-TiO$_2$ composites and P25.

Fig. 8. Effects of NSC–nano-TiO$_2$ composites and P25 on photocatalytic degradation of dye Rhodamine B.

by ultraviolet light with $\lambda_{ex} = 265$ nm, as shown in Fig. 7(b). The PL spectrum intensity of NSC–nano-TiO$_2$ composites is lower than P25, which indicates that recombination is reduced. Electrons are widely distributed on the large surface area of NSC–nano-TiO$_2$ composites, leading to the decrease of the e$^-$/h$^+$ recombination and the increase of the photon efficiency.

3.5. Effects of different catalysts on photocatalytic degradation of dye Rhodamine B

The photodegradation efficiencies of dye Rhodamine B over NSC–nano-TiO$_2$ composites and P25 are illustrated in Fig. 8. The photocatalytic activity of NSC–nano-TiO$_2$ composites is much higher than P25. Firstly, NSC could greatly absorb the organic substance and oxygen of solution because of its large BET surface area. Large BET surface area is attributed to abundant pores in the NSC–nano-TiO$_2$ composites. Dye and oxygen could easily enter into the inner of NSC–nano-TiO$_2$ composites. So dye and oxygen are greatly absorbed on the inner and outer surface of NSC–nano-TiO$_2$ composites. The adsorptive capacity ensures an integrative process from adsorption to reaction, and then separation of reacting agents in the photocatalytic reaction system, thus finally leading to the enhancement of photocatalytic efficiency [21]. After Rhodamine B on NSC–nano-TiO$_2$ composites transfers to TiO$_2$ particles, it is immediately photocatalytically degraded. Secondly, The BET surface area of NSC–nano-TiO$_2$ composites is nearly 15 times larger than P25. As shown in the FESEM micrographs of NSC–nano-TiO$_2$ composites, the average particle diameter of nano-TiO$_2$ is about 10 nm. And according to the calculating formula of BET surface area, the P25 average particle size is about 27 nm. The higher photocatalytic activity of NSC–nano-TiO$_2$ composites may be attributed to the surface effects and the quantum-size effects. Thirdly, oxygen would easily get photogenerated electron from the surface of nano-TiO$_2$ particles in NSC–nano-TiO$_2$ composites to form O$_2^-$ ion. NSC–nano-TiO$_2$ composites for their larger BET surface area would absorb more oxygen than P25. O$_2^-$ ion, which is a good oxidant, could destruct the structure of dye. Therefore, the photocatalytic activity of TiO$_2$ is greatly enhanced by NSC.

4. Conclusion

NSC–nano-TiO$_2$ composites were prepared by sol–gel method. Nano-TiO$_2$ particles were uniformly distributed on the surface of NSC. The photocatalytic activity of NSC–nano-TiO$_2$ composites is much higher than P25. The BET surface area of NSC–nano-TiO$_2$ composites is nearly 15 times larger than P25. NSC could greatly absorb the organic substance and oxygen of solution because of its large surface area.

References

[1] A. Fujishima, T.N. Rao, D.A. Tryk, Titanium dioxide photocatalysis, J. Photochem. Photobiol. C: Photochem. Rev. 1 (2000) 1–21.
[2] A.L. Linsebigler, G.Q. Lu, J.T. Yates, Photocatalysis on TiO$_2$ surfaces: principles, mechanisms, and selected results, Chem. Rev. 95 (1995) 735–758.
[3] B. O'Reganoulos, M. Grätzel, A low cost, high efficiency solar cell based on dye sensitized colloidal TiO$_2$ films, Nature 353 (1991) 737–740.
[4] A. Fujishima, K. Honda, Electrochemical photolysis of water at a semiconductor electrode, Nature 238 (1972) 37–38.
[5] J.K. Zhou, M. Takeuchi, A.K. Ray, M. Anpo, X.S. Zhao, Enhancement of photocatalytic activity of P25 TiO$_2$ by vanadium-ion implantation under visible light irradiation, J. Colloid Interf. Sci. 311 (2007) 497–501.
[6] V. Keller, P. Bernhardt, F. Garin, Photocatalytic oxidation of butyl acetate in vapor phase on TiO$_2$, Pt/TiO$_2$ and WO$_3$/TiO$_2$ catalysts, J. Catal. 215 (2003) 129–138.
[7] K. De Witte, A.M. Busuioc, V. Meynen, M. Mertens, N. Bilba, G. Van Tendeloo, P. Cool, E.F. Vansant, Influence of the synthesis parameters of TiO$_2$–SBA-15 materials on the adsorption and photodegradation of rhodamine-6G, Micropor. Mesopor. Mater. 110 (2008) 100–110.
[8] M.C. Hidalgo, M. Aguilar, M. Maicu, J.A. Navío, G. Colón, Hydrothermal preparation of highly photoactive TiO$_2$ nanoparticles, Catal. Today 129 (2007) 50–58.
[9] M. Tomkiewicz, Scaling properties in photocatalysis, Catal. Today 58 (2000) 115–123.
[10] G. Colón, M.C. Hidalgo, G. Munuera, I. Ferino, M.G. Cutrufello, J.A. Navío, Structural and surface approach to the enhanced photocatalytic activity of sulfated TiO$_2$ photocatalyst, Appl. Catal. B: Environ. 63 (2006) 45–59.
[11] R. Asahi, T. Morikawa, T. Ohwaki, K. Auki, Y. Taga, Visible-light photocatalysis in nitrogen-doped titanium oxides, Science 293 (2001) 269–271.
[12] A. Fuerte, M.D. Hernández-Alonso, A.J. Maira, A. Martínez-Arias, M. Fernández-García, J.C. Conesa, J. Soria, G. Munuera, Nanosize Ti–W mixed oxides: effect of doping level in the photocatalytic degradation of toluene using sunlight-type excitation, J. Catal. 212 (2002) 1–9.
[13] M.C. Hidalgo, S. Sakthivel, D. Bahnemann, Highly photoactive and stable TiO$_2$ coatings on sintered glass, Appl. Catal. A: Gen. 277 (2004) 183–189.
[14] M.C. Hidalgo, D. Bahnemann, Highly photoactive supported TiO$_2$ prepared by thermal hydrolysis of TiOSO$_4$: optimisation of the method and comparison with other synthetic routes, Appl. Catal. B: Environ. 61 (2005) 259–266.
[15] F.B. Li, Q.L. Qian, F. Yan, G.Q. Yuan, Nitrogen-doped porous carbon microspherules as supports for preparing monodisperse nickel nanoparticles, Carbon 44 (2006) 128–132.
[16] Q. Zhao, P. Li, D.Q. Li, X.G. Zhou, W.K. Yuan, X.J. Hu, Synthesis and characterization of titanium silicate-1 supported on carbon nanofiber, Micropor. Mesopor. Mater. 108 (2008) 311–317.
[17] M.M. Mohamed, W.A. Bayoumy, M. Khairy, M.A. Mousa, Structural features and photocatalytic behavior of titania and titania supported vanadia synthesized by polyol functionalized materials, Micropor. Mesopor. Mater. 109 (2008) 445–457.
[18] Y.S. Luo, J.P. Liu, X.H. Xia, X.Q. Li, T. Fang, S.Q. Li, Q.F. Ren, J.L. Li, Z.J. Jia, Fabrication and characterization of TiO$_2$/short MWNTs with enhanced photocatalytic activity, Mater. Lett. 61 (2007) 2467–2472.
[19] X. Yang, L.L. Xu, X.D. Yu, Y.H. Guo, One-step preparation of silver and indium oxide co-doped TiO$_2$ photocatalyst for the degradation of rhodamine B, Catal. Commun. 9 (2008) 1224–1229.
[20] Y.M. Sun, S. Suda, Studies on the fluorination method for improving surface properties and characteristics of AB5-types of hydrides, J. Alloys Compd. 330–332 (2002) 627–631.
[21] Y.Z. Liu, S.G. Yang, J. Hong, C. Sun, Low-temperature preparation and microwave photocatalytic activity study of TiO$_2$-mounted activated carbon, J. Hazard. Mater. 142 (2007) 208–215.